18th Brazilian Congress of Thermal Sciences and Engineering
November 16-20, 2020 (Online)

ENC-2020-0542
ANALYSIS OF PARAMETERS THAT INFLUENCE IN DETERMINING THE CONTACT ANGLE THROUGH IMAGE PROCESSING

Henrique Stacheski Schleetz
Fábio Kenji Suguimoto
Federal University of Technology - Parana (UTFPR) – Alberto Carazzai, 1640, Vila Seugling, Cornélio Procópio – PR, 83600 - 000
hschleetz@alunos.utfpr.edu.br
fksuguimoto@utfpr.edu.br

Marcos Antônio de Souza Lourenço
Federal University of Technology - Parana (UTFPR) – Alberto Carazzai, 1640, Vila Seugling, Cornélio Procópio – PR, 83600 - 000
mlourenco@utfpr.edu.br

Abstract. *Wettability represents a significant parameter in the engineering. Therefore, the development of tools to measure is relevant. Several experimental arrangements can be used, highlighting the sessile drop scheme due to its simplicity. The scheme consists of placing a static drop on a solid surface. Subsequently, photographs are taken, which will be processed to determine the contact angle. The present work aims to evaluate the parameters that influence the measurement of the contact angle through image processing. Therefore, an algorithm for determining contact angles was developed through the software MATLAB® and a series of analyzes was made. Profiles of the experimental drop scheme were artificially created. Through the variation of parameters, such as the value of the contact angles, the curve fit used and the drop shape, it was possible to determine the influence of each variable on the measurement process and on the results. For the spherical drops, the θ/2 method presented an error close to zero for the entire range of contact angles analyzed, while the fitting methods, only for a reduced range. As the flatness of the drop profile increases, an increase in the error also was noted, both for the θ/2 method and for the fitting methods.*

Keywords: *Wettability, contact angle, algorithm, two-phase flow, heat transfer.*

1. INTRODUCTION

Two-phase flow can be defined as the simultaneous flow of two disparate phases inside a tube. The phases can consist either of two distinct immiscible substances and in the same physical state, or of the same substance, however, in different physical states. The main characteristic that differentiates a single-phase flow from a two-phase flow is the formation of flow patterns, existing only in the second. Such patterns refer to the geometric arrangement of the two phases formed during the flow and are relevant for having influence on the heat transfer coefficients and pressure drop values.

According to Shoham (2006), the flow pattern depends on factors such as: the flow rate of each phase, the diameter of the tube, the inclination angle and the physical properties of the two phases (densities, viscosities and surface tensions). An experiment carried out (Takamassa et al., 2008) analyzed the patterns formed for different tube materials, one hydrophilic and one hydrophobic. After the experiment it was found that for different wettabilities, different patterns were obtained, indicating a possible determining factor of wettability for the flow patterns.

The concept of wettability can be defined as the ability of a liquid to maintain contact with the surface of a solid. Currently, the phenomenon has great importance in the industrial sphere, being a relevant parameter for several engineering processes, especially oil recovery, heat transfer and in the two-phase flow itself.

A quantitative indicator of wettability is the contact angle θ formed through the tangent line to the interface point between liquid, solid and air, as shown in Fig. 1.

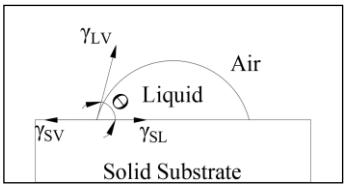

Figure 1. Arrangement of interfacial tensions and contact angle.

The static contact angle θ, also known as Young's angle, is a function of the balance between three interfacial tensions, namely the interfacial tension of the solid-vapor γ_{SV}, the interfacial tension of liquid-vapor γ_{LV} and the interfacial tension of solid-liquid γ_{SL}. The relationship between the angle θ and the tensions can be expressed through Eq. (1).

$$\cos\theta = \frac{\gamma_{SV} - \gamma_{SL}}{\gamma_{LV}} \tag{1}$$

There are several experimental configurations used to measure the contact angle, however, due to its low complexity when compared to the others, the most used is the sessile drop. The method consists of placing a static drop on a solid surface. Subsequently, through image analysis of the profile of the experimental arrangement, it is possible to determine the contact angles. The analysis can be performed using a goniometer, or through image processing methods.

The shape of a sessile drop is defined by the interaction between interfacial tensions and the action of the gravitational force. In the absence of external forces, the drop tends to assume a spherical configuration, because is the arrangement that requires the least surface area and, therefore, the lowest energy level. However, as the volume increases, the effect of the gravitational force becomes evident, flattening the drop profile. A study proposed by Extrand and Moon (2010) demonstrated that for the spherical drop premise to be valid, its volume must be less than 10 μL for drops with contact angle between 10º and 140º.

One of the image processing methods for determining the contact angle is the *θ/2* method, also known as the half angle algorithm. It is assumed that the droplet has a spherical shape and, therefore, that its profile represents an arc of a circle. In such a way, the contact angle can be calculated through Eq. (2) for drops that have contact angles less than 90º, and through Eq. (3) for those that have contact angles greater than 90º, as identified in Fig. 2.

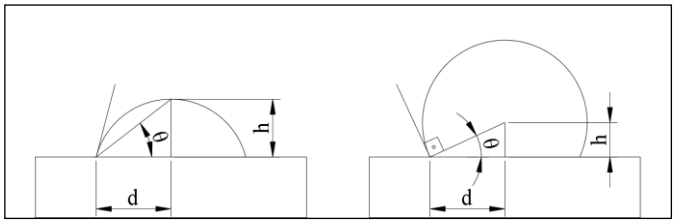

Figure 2. Use of the half-angle algorithm for drops with contact angle less than 90º and for drops greater than 90º.

$$\theta = 2\tan^{-1}\left(\frac{h}{d}\right) \tag{2}$$

$$\theta = 2\tan^{-1}\left(\frac{h}{d}\right) + 90 \tag{3}$$

Rotenberg et al. (1983) were responsible for the development of the Axisymmetric Drop Shape Analysis (ADSA). Basically, the method consists of performing the analysis of the drop profile through the combination of the experimental profile and a theoretical profile found. Surface tension values are necessary for the design of the theoretical profile. The first generation of the Axisymmetric Drop Shape Analysis Profile (ADSA-P) was developed by Rotenberg et al. (1983), and some modifications have been proposed Cheng et al. (1990).

Bateni et al. (2003) presented an automated polynomial adjustment scheme (APF) to determine the contact angles. The coordinates of the droplet profile are extracted using image processing techniques, and then a polynomial adjustment is performed. Finally, the contact angle is calculated through the slope of the polynomial at the interface point between solid, liquid and air.

In this context, it is essential to know the parameters that influence the measurement process and the result of the measured contact angles. To this end, in the present work, an algorithm for determining the contact angles of sessile drops was implemented, and finally, a series of analyzes using artificially generated droplet profiles was carried out in order to evaluate the result of variations in some parameters involved in the process, such as the fit method used and the drop shape.

2. ALGORITHM PREPARATION

An algorithm for determining the contact angles was developed through the software MATLAB®. It is necessary to carry out six major steps after the entry of the original image, namely: Initial Boundaries Tracing, Image Rotation, Image Cut, Analysis and Classification, Separation of Usable Points and, finally, Curve Fit and Calculation of Contact Angles. The graphical representation of the algorithm is shown in Fig. 3.

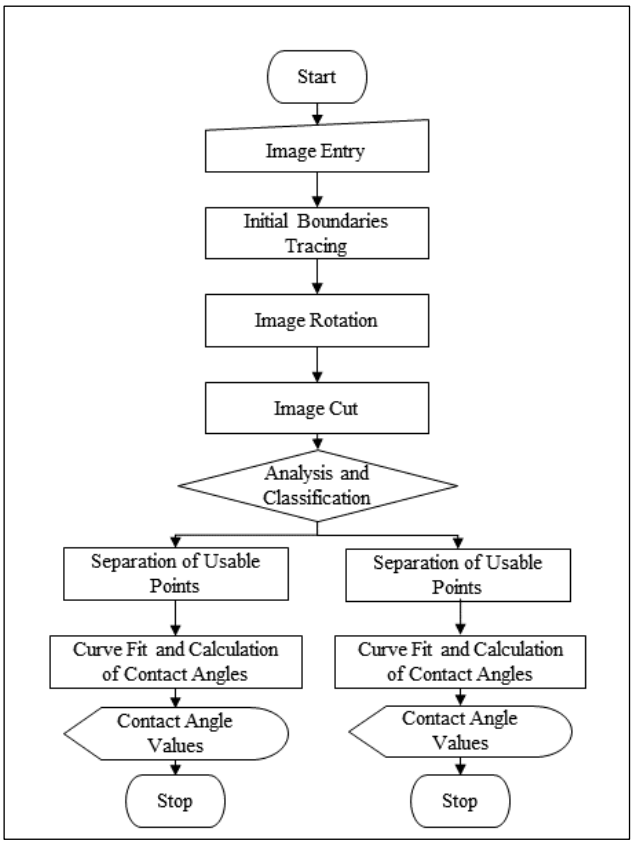

Figure 3. Graphical representation of the algorithm.

2.1 Initial Boundaries Tracing

The initial boundaries tracing consists of the first in a series carried out over the algorithm and has the function of locating the coordinates of the profile of the drop-solid set, which will be used later in the rotation process.

To carry out this step, it is necessary that, previously, the image is binarized. Therefore, the luminance threshold value is calculated using the method of Otsu (1979). All pixels with values greater than the luminance threshold value are replaced by pixels of value 1. In contrast, pixels with values less than the luminance threshold value are replaced by pixels of value 0, completing the binarization process.

After binarization, the colors of the image are inverted, so that the drop-solid set takes on a white color. In some cases, may there reflections in the drop profile. The reflections cause heterogeneities in the inner portion which, in turn, are maintained in the result of binarization. It is necessary, therefore, to perform the internal filling of the profile because the boundaries trace of the limits performed ahead, not only tracks the external boundaries, but also the limits of the internal holes. Such filling is performed through an algorithm based on morphological reconstruction.

Finally, the detection of the drop-solid set limits is performed using the Moore - Neighbor tracking algorithm modified by Jacob's stopping criteria, based in the boundaries function presented by Gonzalez et al. (2004). In Fig. 4 it is possible to observe the different operations carried out in the process.

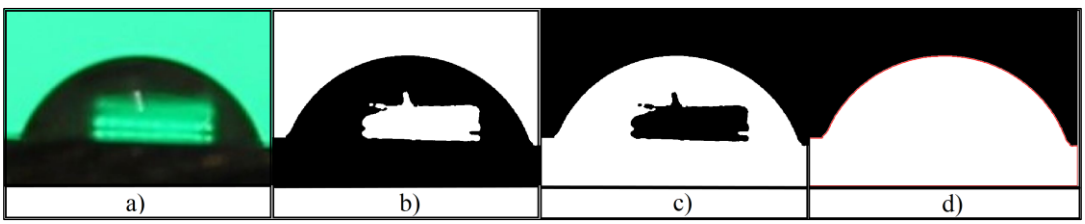

Figure 4. Operations performed in the process of initial boundaries tracing. a) Original image. b) Image after binarization. c) Image after color inversion. d) Image after internal filling; the red lines indicate the localized limits.

2.2 Image Rotation

It is possible that, in the original image, there is an unevenness of the solid, which can be caused either by the unevenness of the camera at the time of taking the photograph, or by the unevenness in the arrangement of the solid. Also, there are cases when is desired to measure the contact angle in conditions where there is a slope of the solid surface. For this purpose, the rotation process aims to correct the possible occurrences described, rotating the image to level it so that there are no errors in the fit and determination of the contact angle process.

The first step of consists of locating, using the data obtained in the previously, the coordinates of the maximum (*Xmax*) and minimum (*Xmin*) values of the upper portion of the solid, measured along the x axis.

Through the two points obtained, the construction of a straight line is carried out, and through its slope the rotation angle is determined. The image is rotated using the nearest neighbor interpolation method. After the rotation, a new limit detection is performed. Fig. 5 shows the images before and after the rotation process.

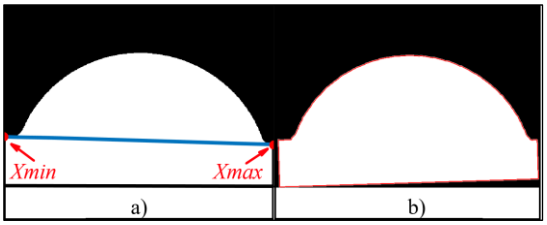

Figure 5. a) Image before the rotation process; the line constructed in blue through points *Xmax* and *Xmin* stands out. b) Image after the rotation process; the red lines indicate the new localized limits.

2.3 Image Cut

After the rotation, the image can be cut to eliminate the profile of the solid, preserving only the drop profile. The cutting step starts from the premise that the surface of the solid is perfectly flat, so that the upper portion of its profile can be represented by the line constructed in the previous step. Thus, the coordinates (*Xc, Yc*) of the minimum value of the upper portion of the solid are located along the x axis and the cut is performed in order to eliminate the entire portion of the image that is below *Yc*. However, in some cases when the solid surface has significant irregularities, the cut made at the height of *Yc* can preserve some portions of the solid. And then, in order to make possible corrections, the program allows the user to enter the value of a cut index *n*, which indicates the number of pixels along the y axis above the level of *Yc* where the cut must occur. It is worth highlighting that *n* must have the smallest possible value due to the fact that the higher the value, more pixels of the droplet profile region are eliminated in the act of cutting, causing inaccuracies in the later stages.

In Fig. 6 the region of the point (*Xc, Yc*) is highlighted, in addition to the graphical representation of index *n*. Also, an image after cutting process is shown.

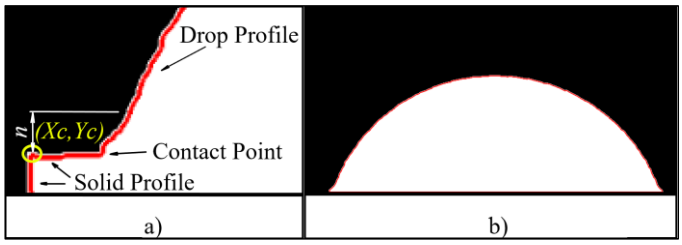

Figure 6. a) Highlighted region of the drop-solid set. b) Image after rotation.

2.4 Analysis and Classification

In this step, an analysis is carried out to classify the profile of the drop among those who have contact angles less than 90º and those who have contact angles greater than 90º. The classification is necessary because, in the future, different points selection processes will be used for the different groups.

Through the data of the boundaries detected previously, the coordinates of the minimum value of the drop profile along the x axis (*Global Xmin*) are located. The coordinates of the minimum value of the drop profile in the region where there is contact with the substrate (*Local Xmin*) are also located. If the value of *Global Xmin* is equal to the value of *Local Xmin*, the drop is classified among those with contact angles less than 90º. If the value of *Global Xmin* is lower in relation to the value of *Local Xmin*, the drop is classified among those that have contact angles greater than 90º.

In Fig. 7 there are two examples of analysis and classification, one from each group. The blue dot represents *Global Xmin*, while the red dot represents *Local Xmin.* Note that for Fig. 7a, the two points are overlapping, classifying the drop among those that have contact angles less than 90º. The opposite is true for Fig. 7b. The value of *Global Xmin* is lower in relation to the value of *Local Xmin*, classifying the drop among those with contact angles greater than 90º.

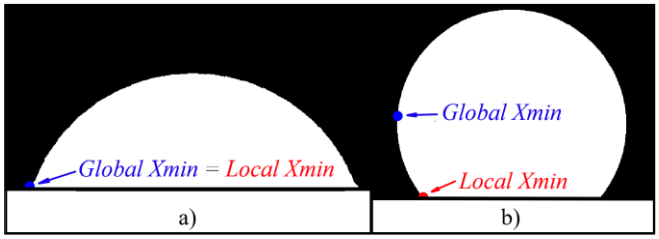

Figure 7. Analysis and Classification for the different groups.

2.5 Separation of Usable Points

After the image classification, it is necessary the selection of the points that will be used in the preparation of the curve fit. Different selection processes are employed for the different groups classified in the previous step.

For drops classified among those that have contact angles less than 90º, it is just necessary to remove the points that represent the contact region between the drop and the solid. To do so, using the same logic as in the previous step, the coordinates of the *Local Xmax* point are located. Thus, the entire region between these points *Local Xmin* (previously located) and *Local Xmax* (located in the current stage) that have the same measured value (*Yc*) along the y axis has its data eliminated.

For drops classified among those that have contact angles greater than 90º, in addition to removing the points that represent the contact region between liquid and solid, it is still necessary to perform the removal of the points that represent the upper portion of the drop, for that the adjustment can be performed without using the polar coordinates system. Therefore, only the region between the *Local Xmin* and *Global Xmin* points is used in the fit step.

In Fig. 8, the blue dots indicate the points that will be used in the fit step, while the red dots indicate those that were discarded.

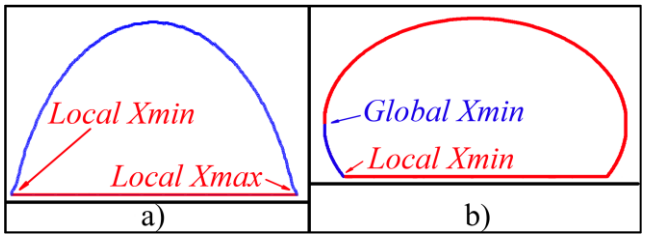

Figure 8. Points that will be used in the fit step for the different groups.

2.6 Curve Fit and Calculation of Contact Angles

After obtaining the points that represent the drop profile, becomes necessary to find a mathematical function that represents it with a certain precision. Therefore, the function must have the same characteristics as the profile, highlighting its inclination at the interface point between air, solid and liquid.

Two possibilities can be considered: the realization of an interpolation, in which the function invariably coincides with all the points obtained, or a curve fit. The second option was chosen, because, in some cases, the juxtaposition of the function on the points obtained would be impossible and it is worth highlighting, that the profile was selected after the binarization process, and not through the original profile, therefore, it would not be interesting to incorporate such variations into a function that seeks to represent the general shape of the drop profile.

Therefore, in the present work, two types of fit were analyzed: the polynomial fit and the fit using the Fourier Series. After the curve fit, the contact angle is calculated using the function derivatives at the contact points. For drops whose contact angle has values less than 90º, two angles are calculated using the derivatives at the *Local Xmin* and *Local Xmax* points and a simple average is calculated to determine θ. For drops whose contact angle has values that 180º, only one value is calculated using the derivative at the *Local Xmin* point. The determination of the contact angle was also performed using the half-angle algorithm, which does not require curve fit.

3. RESULTS AND DISCUSSION

To carry out the analysis of the influence of the drop shape in the process of determining the contact angles, three different profiles were artificially created using CAD software. One, perfectly circular, simulating drops unaffected by the effect of gravity, and the other two ellipticals, simulating drops whose effect of gravity becomes significant. Among the elliptical profiles, were analyzed two different eccentricity values ($e_1 = 0{,}80$ and $e_2 = 0{,}98$), to represent two levels of flatness of the drop profile.

The use of artificial profiles allows the analysis a wide range of contact angles, in addition to the possibility of comparing the value of the angle obtained with the real value, previously defined in the preparation of the profile.

The analyzes were performed considering different types of curve fit, among them the polynomial (of 2, 4, 6, and 8 degrees) and the fit via Fourier Series (of 1, 3, 5 and 7 terms). Furthermore, the contact angles were also determined using the geometric method *θ/2*. For each result obtained through different methods, the absolute error values were determined using Eq. (4). Finally, the absolute error values were plotted in graphs in function of the contact angle.

All analyzes were performed with $n = 2$.

$$\mathrm{E_{abs}} = |\theta - \text{real value}| \tag{4}$$

3.1 Circular profile

For drops with a circular profile with contact angles below 90°, Fig. 9a represents the absolute error in function of the contact angle for calculations using the polynomial fit, and Fig. 9b for calculations using the fit via Fourier Series. The two methods were compared with the results obtained using the *θ/2* method.

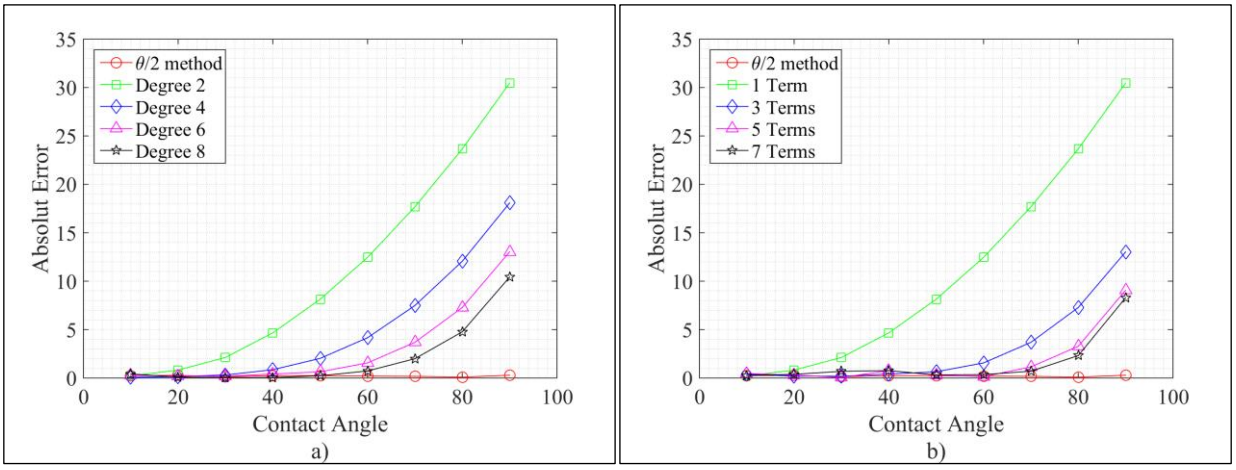

Figure 9. Analysis for drops with a circular profile with contact angles below 90°.

It can be seen in Fig. 9a that the polynomial fit showed increasing error values, as the contact angle increases. It is worth mentioning that, with the increase in the degree of the polynomial, there is also a decrease in the error values, especially for the initial values of the contact angles, with the 8th degree polynomial having the least errors. For the adjustment made through the Fourier Series (Fig. 9b), in essence, the same behavior is observed. There is an increase in the error as there is an increase in the contact angles, in addition, there is a decrease in the error values as there is an increase in the quantity of terms of the adjustment, with the fit of 7 terms presenting minor errors.

For drops with a circular profile with contact angles above 90°, Fig. 10a represents the absolute error in function of the contact angle for calculations using the polynomial fit, and Fig. 10b for calculations using the fit via Fourier Series. The two methods were compared with the results obtained using the *θ/2* method.

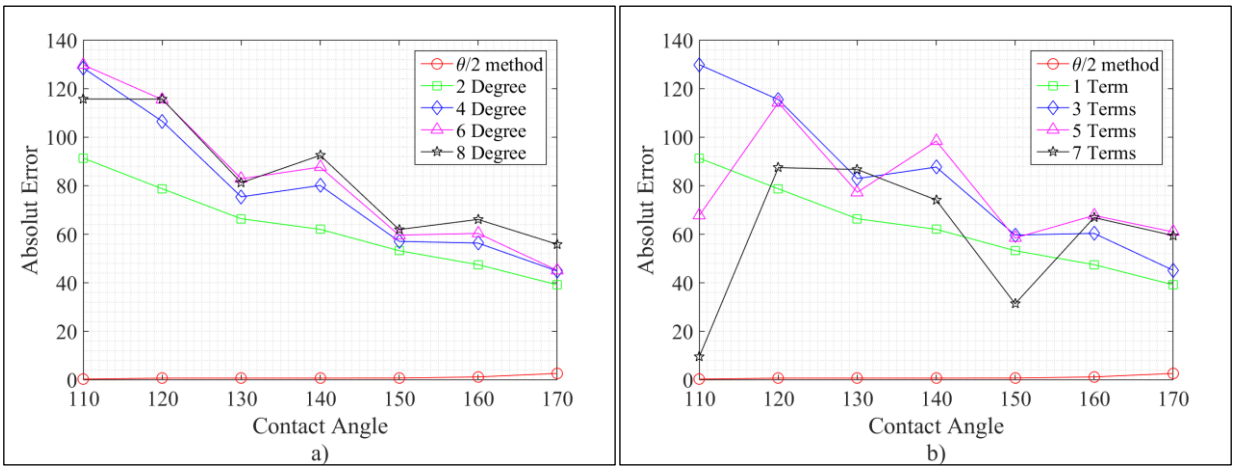

Figure 10. Analysis for drops with a circular profile with contact angles above 90°.

It can be seen in Fig. 10a that the polynomial fit presents high error values (with a minimum value of 39.2°, in the case where a two-degree curve is fitted for the drop whose contact angle is 170°), in addition to a tendency to decrease the error as the contact angles increase. The high value is due to the fact that, for drops whose contact angle has a value greater than 90º, the portion of the usable points selected has a low number of points, compromising the curve fit. Furthermore, it is possible to explain the tendency to decrease the error based on the fact that, with the increase in contact angles, a larger portion of the drop is selected, increasing the number of points used in the curve fit. Finally, it is possible to notice a decrease in error with a decrease in the degree of the polynomial.

Analyzing the fit made with the Fourier Series (Fig. 10b), in addition to the high error (with a minimum value of 9.7°, in the case where a fit of seven terms is performed for the drop whose contact angle is 110°) , it is also possible to observe greater instability in the results. However, the same patterns that exist in polynomial adjustment, in short, can also be seen in the fit via Fourier Series.

The *θ/2* method proved to be consistent, with an error close to zero for the entire range of contact angles analyzed, showing a slight upward tendency in cases where θ assumes values greater than 160°, due to inaccuracies in the preparation of artificial profiles, which become more significant in that region. It is worth noting that the maximum error presented by the method *θ/2* has a value equal to 2.6° and is manifested in the case where the drop has a contact angle equal to 170°.

3.2 Elliptical profile 1

For drops with an elliptical profile ($e_1 = 0{,}80$) with contact angles below 90°, Fig. 11a represents the absolute error in function of the contact angle for calculations using polynomial fit, and Fig. 11b for calculations using fit via Fourier Series. The two methods were compared with the results obtained using the *θ/2* method.

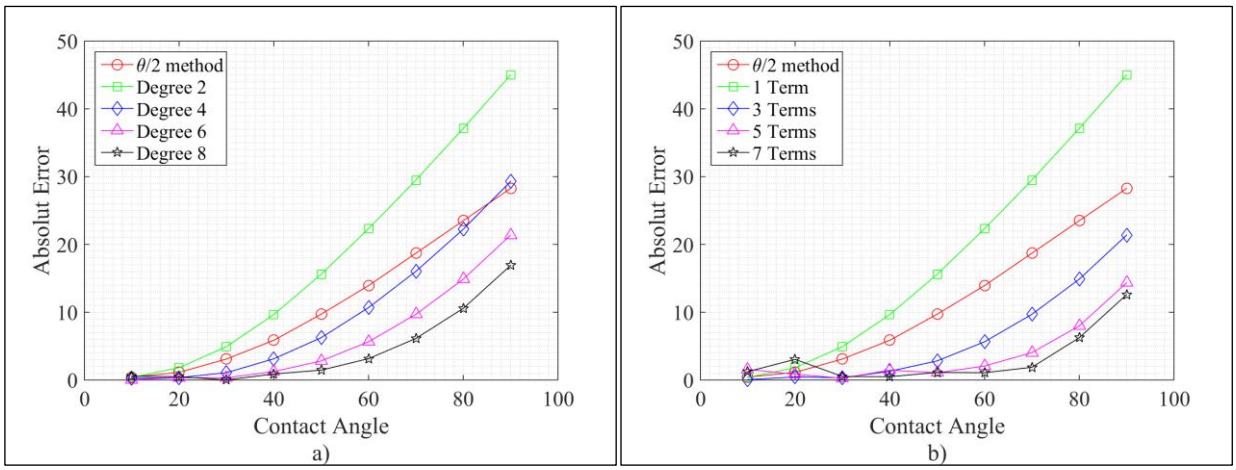

Figure 11. Analysis for drops with an elliptical profile 1 ($e_1 = 0{,}80$) with contact angles below 90°.

The behavior observed both for the polynomial fit (Fig. 11a), and for the fit via Fourier Series (Fig. 11b), is very close to observed for the same range of angles in circular profiles. However, a substantial increase in error is noted when the contact angles are determined using the *θ/2* method. This behavior can be explained by the fact that the *θ/2* method is purely geometric, based on a perfectly circular profile.

For drops with an elliptical profile ($e_1 = 0{,}80$) with contact angles above 90°, Fig. 12a represents the absolute error in function of the contact angle for calculations using polynomial fit, and Fig. 12b for calculations using fit via Fourier Series. The two methods were compared with the results obtained using the *θ/2* method.

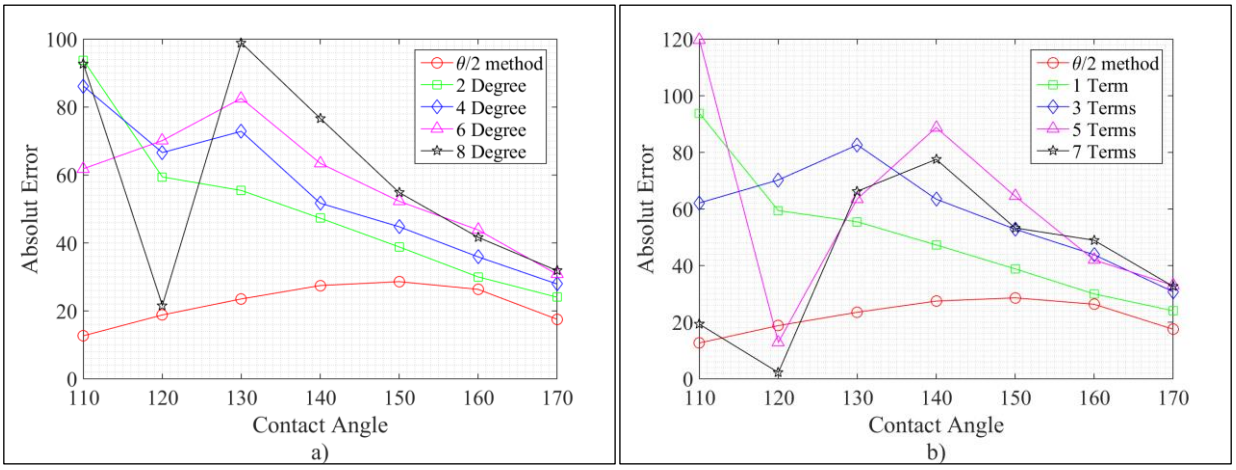

Figure 12. Analysis for drops with an elliptical profile 1 ($e_1 = 0{,}80$) with contact angles above 90°.

The results obtained with polynomial fit (Fig.12a), and with the fit via Fourier Series (Fig. 12b) showed unstable behavior and high error values, with a slight tendency to decrease as the contact angles increase. The results using the *θ/2* method also showed high error values, reaching a maximum value of 28.6° when measured for drops whose contact angles are equal to 150°.

3.3 Elliptical profile 2

For drops with an elliptical profile ($e_2 = 0{,}98$) with contact angles below 90°, Fig. 13a represents the absolute error in function of the contact angle for calculations using polynomial fit, and Fig. 13b for calculations using fit via Fourier Series. The two methods were compared with the results obtained using the *θ/2* method.

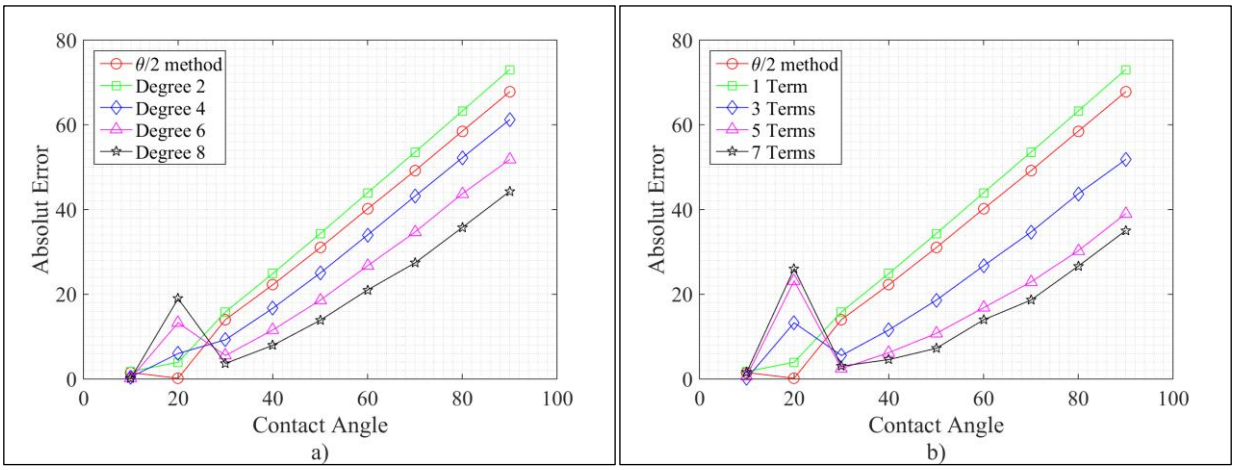

Figure 13. Analysis for drops with an elliptical profile 2 ($e_2 = 0{,}98$) with contact angles below 90°.

Note in Fig.13a and Fig. 13b, in short, the same patterns observed previously for contact angles below 90°, except for the behavior shown for angles up to 20°. In these cases, there is an increase in the error as there is an increase in the polynomial degree or in the quantity of terms of the fit with Fourier Series, a fact that changes with the increase of the contact angles, returning to patterns previously seen. This behavior is explained based on the idea that there is a high flatness for small contact angles, which makes the profile better represented by polynomial fits with lesser degrees and

fits via Fourier Series with smaller amounts of terms. As the contact angle increases, the flattening decreases, and the curves of greater degree or greater number of terms start to show the smallest errors.

For drops with an elliptical profile ($e_1 = 0{,}98$) with contact angles above 90°, Fig. 14a represents the absolute error in function of the contact angle for calculations using polynomial fit, , and Fig. 14b for calculations using fit via the Fourier Series. The two methods were compared with the results obtained using the *θ/2* method.

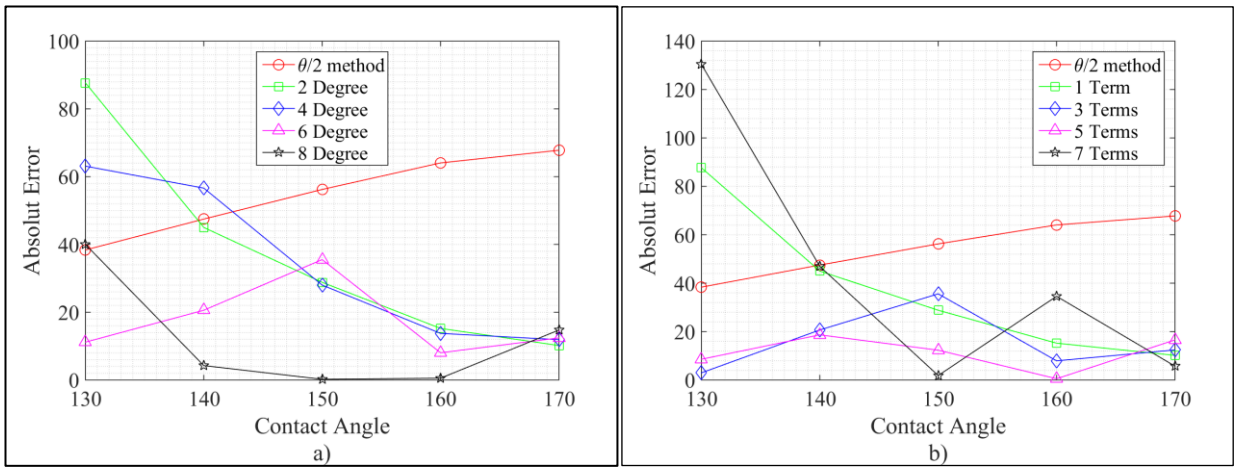

Figure 14. Analysis for drops with an elliptical profile 2 ($e_2 = 0{,}98$) with contact angles above 90°.

It can be seen in Fig.14a and Fig. 14b that both the polynomial fit and the fit via Fourier Series presented unstable results and high error values, despite a tendency to decrease them. The results obtained using the *θ/2* method also showed high errors, in addition to an increasing tendency, as there is an increase in contact angles, registering its lowest value (38.4°) for the case which the drop has contact angles equal to 130°. It is noteworthy that, due to the low number of points selected for the curve fit step, the images that corresponded to values greater than 100° and less than 130° were not possible to be processed.

4. CONCLUSION

After the development of the image processing algorithm, aimed to determining the contact angles, sought to determine the influence of the curve fitting method on the final result. Three different profiles, representing different types of drops, were also analyzed for the range from 10º to 170º. Finally, the absolute error of each measurement was calculated, and these results were analyzed in function of the contact angles.

After analyzing the results, it can be concluded that, for the spherically shaped drops, the determination of the contact angles using the *θ/2* method presented the lowest absolute error values for the entire analyzed range. The *θ/2* method also requires less computational resources when compared to the curve fit used, configuring the most efficient method among those analyzed in the present work. It is worth mentioning that, despite requiring greater computational resources, the fitting methods also have applicability for restricted intervals. The polynomial adjustment of 8 degrees showed values close to zero for contact angles below 60°, presenting for this interval the maximum value of 0.73° of absolute error. In addition, the adjustment using the Fourier Series of 7 terms can also be applied for contact angles below 70º, with a maximum value of 0.70° for this interval.

For elliptical shaped drops with eccentricity equal to 0.80, it is noted that the *θ/2* method loses efficiency, presenting high error values. The application of fitting methods also has a reduced application interval, making it possible to use the 8-degree polynomial fit for contact angles below 40°, presenting, for this interval, the maximum value of 0.89° of absolute error. The fit via Fourier Series of 7 terms also showed some error values close to zero for contact angles below 40°, registering the minimum value of 0.49° for this interval, however, the instability of the results makes its impracticable.

For elliptical shaped drops with eccentricity equal to 0.98, it is noted that any method of determining contact angles presented low values of absolute error, making all three methods studied unfeasible for this kind of analysis.

5. ACKNOWLEDGEMENTS

I thank my supervising teacher Fábio K. Suguimoto for his patience and guidance, and to UTFPR for the opportunity.

6. REFERENCES

Bateni, A., Susnar, S.S., Amirfazli, A., Neumann, A.W., 2003. "A high-accuracy polynomial fitting approach to determine contact angles". *Colloids and Surfaces,* Vol. 219, pp. 215-231.

Cheng, P., Li, D., Boruvka, L., Rotenberg, Y., Neumann, A.W., 1990. "Automation of axisymmetric drop shape analysis for measurements of interfacial tensions and contact angles". *Colloids and Surfaces,* Vol. 43, pp. 151-167.

Extrand, C. W., Moon, S. I., 2010. "When sessile drops are no longer small: transitions from spherical to fully flattened". *Langmuir,* Vol 26, pp. 11815 – 118822.

Gonzalez, R. C., R. E. Woods, and S. L. Eddins, 2004. *Digital Image Processing Using MATLAB,* New Jersey, Pearson Prentice Hall.

Otsu, N., 1979 "A Threshold Selection Method from Gray-Level Histograms." *IEEE Transactions on Systems, Man, and Cybernetics.* Vol. 9, No. 1, 1979, pp. 62–66.

Rotenberg, Y., Boruvka, L., Neumann, A.W., 1983. "Determination of Surface Tension and Contact Angle from the Shapes of Axisymmetric Fluid Interfaces". *Journal of Colloid and Interface Science,* Vol. 93, pp. 169-183.

Shoham, O., 2006. *Mechanistic Modeling of Gas-Liquid Two-Phase Flow in Pipes.* Society of Petroleum Engineers

Takamasa, T., Hazuku, T., Hibiki, T., 2008. "Experimental Study of gas–liquid two-phase flow affected by wall surface wettability". *International Journal of Heat and Fluid Flow,* Vol 29, pp. 1593 – 1602.

7. RESPONSIBILITY NOTICE

The authors are the only responsible for the printed material included in this paper.